THEORETICAL AND EXPERIMENTAL RESEARCH REGARDING THE AERODYNAMICS OF A SHIP SAIL SYSTEM

C. BERBENTE, C. MARALOI*

Se studiază o configuraţie de vele hibridă, alcătuită dintr-un catarg profilat, o pânză impermeabilă şi un volet de bord de atac. În acest fel, se obţine un sistem cu performanţe ridicate pentru propulsia navelor. Studiul cuprinde o parte analitică, una numerică şi alta experimentală. Pentru modelul analitic, se foloseşte conceptul de linie portantă (Prandtl) aplicat unei aripi "în oglindă", şi o metodă proprie de determinare a coeficienţilor circulaţiei, capabilă să preia stabil salturile de coardă.

Pentru modelarea numerică, se utilizează un cod bazat pe metoda elementelor finite. Experimentele s-au efectuat în tunelul Academiei Navale din Constanţa.

A configuration of a hybrid sail consisting of a solid mast, a peremeable flexible part and a leadig edge flaps is studied. On this way one obtains a high performance system for ship propulsion. The study includes an analytical, a numerical and an experimental part. For the analytical part a Prandtl lifting line model is used, applied to a „wing in mirror". An original method capable to take into account chord jumps is used to determine the coefficients of circulation. For the numerical modelling a finite element code is applied. The experiments were carried-out at the Constantza Naval Academy wind tunnel.

1.Considerations on hybrid sails.

The aerodynamic characteristics of simple sails, as well as the aerodynamic characteristics of sails installed on round masts are already studied both theoreticaly and experimentaly.

Combinanations consisting of a peremeable flexible part and a leadig edge slat, an assembly named here *hybrid sail* (Fig.1), are less studied.

* Prof., Dept. of Aerospace Sciences "E.Carafoli"-University „Politehnica"of Bucharest.; Chair of Nautical Sciences "Ghe. Balaban" – Naval Academy "Mircea cel Bătrân", Constanta

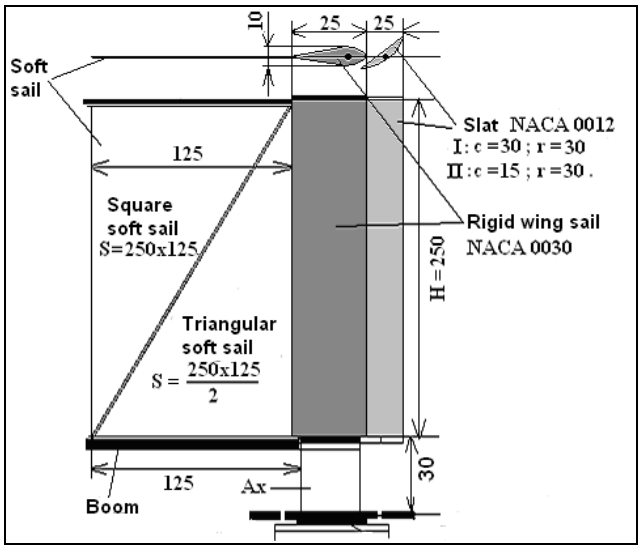

Fig.1. The hybrid sail model

2.1 The lifting line theory.

In the following one presents a method based on the Prandtl lifting line concept,extended to a finite span wing with a slat and a flexible but impermeable part.The flexible (soft) part ia deformable wing, which is curved under the pressure difference between upper side and lower side. Its planform could be triangular, rectangular or even elliptical.

The following notations are used (Fig.2): Cc – mast chord;Cb – sail chord (base); Cv –slat chord; C_e – chord at extremity y = b/2; C_0 – chord at y = 0; ε – sail distance to ship deck; b/2 – hybrid sail halfspan; a.p.n. –zero lift axis;

ω_V –slat angle; β –boom angle; α_0 – stream angle of attack with respect to a.p.n.; α_g –the geometrical angle of attack; V∞ -velocity at upstream infinity.

The slat will be considered a rigid rectangular wing.

The deck will be treated like a solid infinit wall; its influence will be taken into account by a „ ***wing in a mirror"*** .AS a cosequence, the resulting motion takes place around a wing having a double span b.

According to Prandtl's lifting line concept, one replaces the sail-mast-slat system by a vortex line of intensity Γ (Fig.2), from which a free vortex sheet is generated, lain on the stream and extended to downstream infinity.

One can write the following relations:

$$\Gamma = kcV_\infty \alpha_e \,, \qquad (1\text{-a})$$

where c is the total chord:

$$c = c_b + c_c + p_r c_v\,,\ k \cong 0{,}9\pi\,, \tag{1-b}$$

α_e being the effective angle of attack:

$$\alpha_e = \alpha_0 - \alpha_i\,, \tag{2}$$

where:
- α_0 = the angle of $V_{\infty,}$ with respect to a.p.n.
- α_i = the deviation angle induced by the free vortex sheet (parallel to V_∞).
- p_r percentage of the slat not overleapping the mast.

The proposed model is simplified, but able to take into account two important effects: a) the slat angle, ω_v (Fig. 2); b) the sail curvature. One considers that outside of a small region in the neighbourhood of zero-lift flow, the position of a.p.n. changes very little with respect to the hybrid sail system at a fixed slat angle. This assumption can be verified by an almost constant slope of the lift coefficient as a function of α_0. It tourns out from the comparison between theory and experiment that this assumption is correct. Further by introducing the angle θ defined as follows:

$$y = -\frac{b}{2}\cos\theta\,,\ \theta \in [0, \pi]\,, \tag{4}$$

one obtains for thecirculation Γ at a station y of the hybrid sail system the expression:

$$\Gamma = 2bV_\infty \sum_{p=1}^{\infty} A_p \sin p\theta\,, \tag{5}$$

A_p being coefficients to be determined by introducing the series (5) in equatin (1).

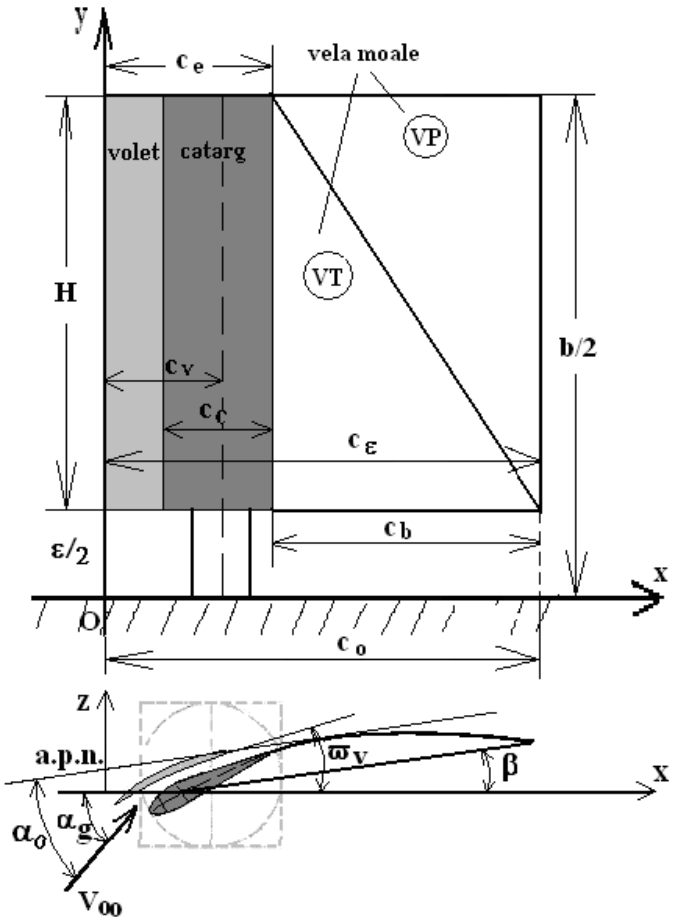

Fig. 2. The rectangular hybrid sail (VP) and the triangular hybrid sail (VT).Parameter deffinition.

Taking into account the expression of the indesed angle α_i :

$$\alpha_i = \sum_{p=1}^{\infty} \frac{pA_p \sin p\theta}{\sin\theta}, \tag{6}$$

Prandtl equation (1) becomes:

$$\sum_{p=1}^{\infty} A_p \sin p\theta = \mu\left(\alpha - \sum_{p=1}^{\infty} \frac{pA_p \sin p\theta}{\sin\theta}\right) \cdot \ (\mu = kc/2b\ ). \tag{7}$$

Under the form (7) the determination of the coefficients A_p, $p = 1,2,3...$, meets certain difficulties, both for the calculul analytical and numerical (with one

exception: c ~ sin θ, elliptical wing), due to instabilities at end stations: θ = 0 and θ = π.To avoid these difficulties we will use the method given in [2].

Indeed, by multiplieing the ecuation (7) with sin(nθ), n = 1,2,3…., then integrating it from θ = 0 to θ = π ,one obtains the following system of ecuations:

$$\left(\frac{\pi}{2}+nH_{nn}\right)A_n = I_n - \sum_{p=1}^{\infty} pH_{np}A_p \ , \qquad (\text{n} = 1,2,3\ldots..) \ , \tag{8}$$

where I_n şi H_{np} are the integrals:

$$I_n = \int_0^{\pi} \mu\alpha \sin n\theta d\theta \ ; \ H_{np} = H_{pn} = \int_0^{\pi} \frac{\mu \sin n\theta \sin p\theta}{\sin\theta} d\theta \ , (p,n = 1,2,\ldots) \tag{9}$$

The wing and incidence $\alpha(\theta)$ being symmetrical one yields:

$$\mu(\theta) = \mu(\pi-\theta) \ , \text{şi } \alpha(\theta) = \alpha(\pi-\theta) \ , \tag{10-a}$$

$$H_{np} = 0 \ , \text{ for } n + p = \text{odd}, \tag{10-b}$$

$$I_n = 0 \ , \ n = 2p = \text{ even}. \tag{10-c}$$

A consequence a relațiilor (10.a,b,c) is the vannishing of the coefficients A_n for n even:

$$A_{2m} = 0 \ . \tag{11}$$

Dann one needs the system (8) odd indices in the form [2]:

$$L_{2m-1}A_{2m-1} = I_{2m-1} - \sum_{\substack{p=1, \\ p\neq m}}^{\infty} (2p-1)H_{2m-1,2p-1}A_{2p-1} \ , \tag{12}$$

where :

$$L_n = \frac{\pi}{2} nH_{nn} \ . \tag{13}$$

Under assumpsion (subsequently confirmed) of a rapid convergence of series (5) of the circulation, we neglecti in (12) terms A_{2m+3} as compared A_{2m-1} (four indeces distance).

On the other hand, the integrals $H_{2m-1,2p-1}$ are decreasing with the indices m, p, due to alternate sign of functions $\sin(2m-1)\theta$ şi $\sin(2p-1)\theta$ in the interval [0,π]. For these reasons one may truncate the infinite summ in (12), starting with $p = m + 2$.

Thus we can restrict ourselves to calculat only the coefficients A_1 şi A_3:

$$A_1 = \frac{I_1 L_3 - 3 I_3 H_{13}}{L_1 L_3 - 3 H_{13}^2}\ ;\ A_3 = \frac{1}{L_3}\left(I_3 - H_{31} A_1\right). \tag{14}$$

If one desires a better accuracy, one can start with three coefficients: A_1, A_3, A_5, using three ecuations obtaind for m =1; 2; 3.

Knowing rhe coefficients A_1, A_3,…, one can calculate the aerodynamical forces.

The lift coefficient, C_z, is:

$$C_z = \pi \lambda A_1\ ,\quad \lambda = \frac{b^2}{S}\ . \tag{15}$$

A_1 being given by relation (14).

The coefficient of the induced aerodynamical drag , C_x , is:

$$C_{xi} = \frac{C_z^2}{\pi \lambda} \sum_{n=1}^{\infty} n \frac{A_n^2}{A_1^2} \approx \frac{C_z^2}{\pi \lambda}\left(1 + 3\frac{A_3^2}{A_1^2}\right). \tag{16}$$

2.2. Generale formulele of integrals I_{2m-1}, $H_{2m-1,\ 2p-1}$, case $\varepsilon \neq 0$ (Fig.2) .

In fact there is a distance ε/2 between sail basis (boom) and deck. This will introduce a new jump in the chord distribution. Again the proposed method [2] is to be recommanded. By denoting with β_ε the corresponding angle, one gets ($y = \frac{\varepsilon}{2}$):

$$\sin \beta_\varepsilon = \frac{\varepsilon}{b},\ \beta_\varepsilon = \arcsin \frac{\varepsilon}{b} \in \left[0, \frac{\pi}{2}\right]\ . \tag{17}$$

Integrals along the wing span $\left(\theta \in [0, \pi]\right)$, are calculated by extracting the portion (-ε/2, ε/2) out of a complet wing.

We have calculated the required integrals in amore general case, for a trapezoidal wing, at invariable incidence, α_0. Then one gets as particular cases the rectangular and the triangular wings. The siplest case corresponds to ellipticl wing. For the symmetrical wing the chord parameter variation, μ, defined by relation (7):

$$\mu = \frac{kc}{2b} = \mu_0\left[1 - r\left|\cos\theta\right|\right]; \quad \mu_0 = \frac{kc_0}{2b}; \quad r = 1 - \frac{c_e}{c_0} \quad , \tag{18}$$

r being the trapezoidality ratio: c_e = chord at extremity y = b/2, c_0 = chord at y = 0.

Thus, one obtains for the integrals I_{2m-1}, defined by relation (9), the expressions:

$$\frac{I_1}{\mu_0\alpha_0} \equiv I_{1r} = 2(1-\sin\beta_\varepsilon) - r\cos^2\beta_\varepsilon; \tag{19}$$

$$\frac{I_3}{\mu_0\alpha_0} \equiv I_{3r} = \frac{2}{3}\left(1+\sin 3\beta_\varepsilon\right) - r\left(1+2\sin^2\beta_\varepsilon\right)\cos^2\beta_\varepsilon, \tag{20}$$

index „r" standing for „raported".

The other integrals are expressed as functions of I_{1r} şi I_{2r}, as follows:

$$L_1 = \frac{\pi}{2} + \mu_0 I_{1r} \; ; \quad L_3 = \frac{\pi}{2} + 3\mu_0 H_{33r}; \tag{21}$$

$$H_{33r} = I_{3r} + 2\left(\frac{6}{5} - \frac{\sin^2 5\beta_\varepsilon}{5} - \sin\beta_\varepsilon\right) - r\left(\frac{4}{3} - \frac{\sin^2 3\beta_\varepsilon}{3} - \sin^2\beta_\varepsilon\right). \tag{22}$$

Now one can calculate the first three coefficiens of circulation:

$$\frac{A_1}{\mu_0\alpha_0} \equiv A_{1r} = \frac{I_{1r}L_3 - 3\mu_0 I_{3r}^2}{L_1 L_3 - 3\mu_0^2 I_{3r}^2}; \quad A_2 = 0; \tag{23-a}$$

$$\frac{A_3}{\mu_0\alpha_0} \equiv A_{3r} = \frac{I_{3r}}{L_3}\left(1 - \mu_0 A_{1r}\right). \tag{23-b}$$

We have taken in consideration two cases:

a) the square hybrid sail, both with big slat (VP1a) and small slat (VP2a);
b) the triangular hybrid sail , with big slat (VT1a) and small slat (VT2a).

The resultat of the analytical calculations and comparisons with experiments are given in Table 1 and 2.

Table 1.

Comparisons analytical model –experiment for the slope of lifting coef. C_Z

Model	r	μ_0	λ	A_{1r}	A_{3r}	$\frac{dC_Z}{d\alpha_0}$ (grad^{-1})	
						theory	exper.[4] (min error.)
VP1.a.	0.	0.4298	3.689	0.7078	0.1164	0.0614	0,0682 (9.94%)
VP2a	0.	0.4030	3.920	0.7208	0.1235	0.0627	0.682 (8.09%)
VT1.a	0.7568	0.4670	5.834	0.5027	0.0276	0.0751	0,0789 (4.82%)
VT2a	0.8000	0.4418	6.491	0.4941	0.0185	0.0769	0.0769 (0.0%)

As a conclusion, the lifting line theorie is applicable for angle of attack α_0 corresponding to interval (C_{Zmin}, C_{Zmax}).

The angle α_0 is measured with respect to a.p.n. of the hybrid sail system and depends on the curbature of the profil „ profiled mast-soft sail- slat". Although this dependence is complicate, one can assume a pretty constant slope of the curve $C_z(\alpha)$ for a fixed configuration.

Table 2.

Comparisons analytical model – experiment for *Cx la Czmax*

Model	*α (dgr) Cz = 0*	*α d(gr) Czmax*	*δα (dgr)*	*Czmax (dgr)*	α_{imax} *(grd)*	*Cx la Czmax*	
						theory (indus)	*experiment[4]*
VP1.a.	-23,5	7.0	30.5	2.05	10.41	0,372	0,650 (57.2%)
VP2.a	-23.0	8.0	31.0	2.25	10.77	0.423	0.750 (56.4%)
VT1.a	-12.7	18.0	30.7	2.25	7.05	0,277	0,500 (55.4%)
VT2.a	-12.0	17.0	29.0	2.50	7.10	0.310	0.500 (62.0%)

Thus, the good agreement between theorie and experiment for the slope $dC_Z/d\alpha_0$, the four cases presented in Table 1, especially for larger values of the aspect ratio λ, suggest a linear variation of C_Z with α- the angle between the

relative speed $V_{vr,}$ with the rigid mast profiled as awing. Therefore the assumption of a almost unmodified direction of the a.p.n. direction is confirmed. In exchange,one may see a significant displacement of a.p.n. with wing wing planform, but not with the slat chord. As well angle α_0 at Czmax keeps a value around 30degree.(Table 2). As regards the drag coefficient, *Cx*, at Czmax, more than a half (cca 60%) is induced by the free vortex sheet, the rest belonging to frection effects.

The two times increas of the angle $\alpha_{0\ max}$ in comparison to usual wings can be explained through the slat effect as well by flexible wing adaptation to flow (Table 2).

The proposed method for solving the Prandtl equation, has the followiing advantages:

- it takes into account without problems the sudden chord variations or jumps (four jumps in our case, for the „wing in mirror";
- permits an exact calculatins of the integrals leading to simple analytical exprsesions;
- a rapid convergence, the coeficiens A_1 *şi* A_3 $(A_2=0$ *şi* $A_4=0)$ giving a good accuracy .

3. Use of finite element method for determining the parameters of triangular hybrid sail.

The equations governing the fluid motion are the continuity equation, the Navier-Stokes equations (expressing the momentum conservation) and the energy equation. (expressing the fluid energy conservation). Excepting some particular cases, the set of equations cannot be solved analytically. To solve this system of partial-differential equations one uses various numerical codes, among them one of the most elaborated is FLUENT.

In the following, we shall use the code **Cosmos FloWorks**, a simpler code permitting both cantitative evaluations and the visualization of flow field in 2D and3D, by using the finite element method.The outputs of **CosmosFloWorks** contain node values of speed, pressure, temperature etc. The graphical display of these results can be performed by **SolidWorks** program. This includes the possibility of plotting in colors the stream lines, of pressure distribution, of temperature and of shear; it can plot the speed vectors as well. To analyse with finite elements, in case of triangular sailpatterns (VT) and rectangular ones (VP) the SolidWorks Professional program was used.Tests were performed in the following conditions:

- standard incompressible air (20^0C, 770mm Hg);
- the current motion is considered to be steady;
- the sail roughness isn't taken into account;

- the wind angle of attack, depending on the case, was of 30^0 and 45^0.

3.1. The triangular hybrid sail VT.

The pressure field of the triangular sail VT1.a) subject to a current of 12 m/s and an attack angle of 30^0 is shown in Fig.3.By analysing Fig.3, it resulted that the pressure on 1/3 of the slat chord has a value near to the atmospheric pressure, the rest of 2/3 being subject to reduced pressures, which will induce an increase of air current speed on the upper side of the system, but on the other hand, the peak pressures are induced on the hard wing and the soft sail, specially at the leading edge; the difference between these values determines the increases of buoyancy.

The field of speeds of triangular sail VT1.a) shown in Fig. 4, is subject to a current of 12 m/s and an attack angle of 30^0. From the analysis of Fig. 4, it has

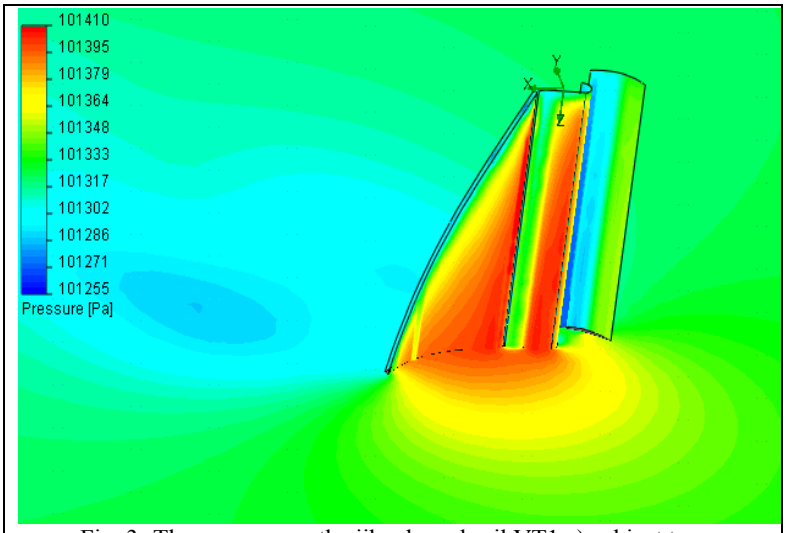

Fig. 3- The pressure an the jib- shaped sail VT1.a) subject to a flow/stream of 12m/s, and an angle of attack of 30°.

been found that the current speed is low on the lower side of hybrid sail, even achieving the stagnation , that will determine a very high pressure on the lower side. The current in excess is overflown to the upper side of the system inducing ascendent (anabatic) currents.To the trailing edge the current speed is reduced tending to be equal to the general speed. The influence of slat can be seen in this figure, because the current speed increased on the upper side of hybrid sail, from 12 m/s to 15 m/s, especially to the bow, where a very big difference of speed, from 15 m/s to 1,5 m/s, induces an accelerated flow determining a large difference of pressure and leading to an increase of propulsion.

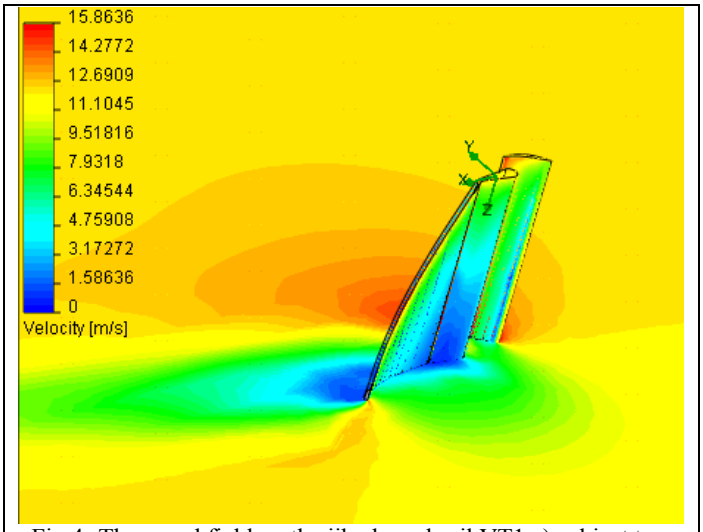

Fig 4- The speed field on the jib-shaped sail VT1.a) subject to a flow/stream of 12m/s, and an angle of attack of 30°.

3.2. The rectangular hybrid sail VP.

The pressure field of the triangular sail VP1.a), shown in Fig.5, is subject to a current of 12 m/s and an angle of attack equal to 45^0. From the analysis of Fig. 5 it results that the pressure on the lower side of the system is higher as compared to the upper side of it, this difference being produced and kept by the position and the orientation/direction of the slat. Having entrapped the air current in the first two thirds of the chord, the slat increases the pressure of the system; further there

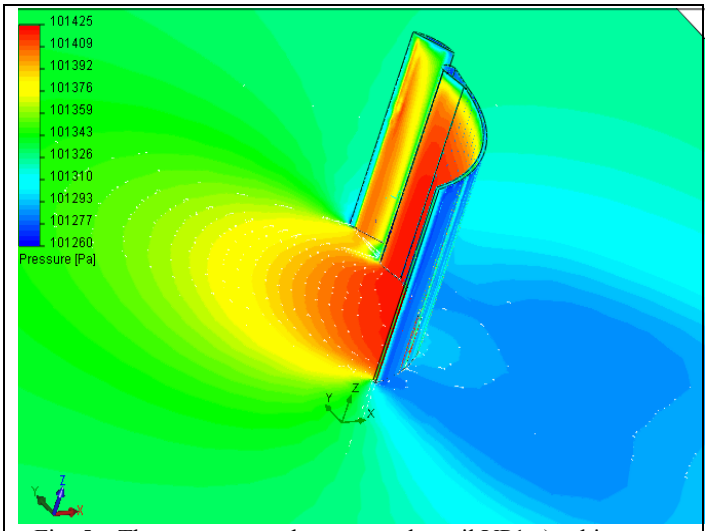

Fig. 5 – The pressure on the rectangular sail VP1.a) subject to a flow/stream of 12m/s and an angle of attack of 45°.

is a decrease of the pressure in the last chord third, resulting an acceleration which leads to an increase of the current speed at the outlet through the slot created between the slat and the profiled wing. This increase of the speed will raise the depression (negative pressure) on the upper side, so increasing the upward force.

The field of speeds of triangular sail VP1.a), shown in Fig. 6, is subject to a current of 12 m/s and an attack angle of 45^0. From the analysis of Fig. 6, it has been found that the current speed is low on the lower side of hybrid sail, also achieving the the stagnation, that will determine a very high pressure on the lower side. The current in excess is overflown to the upper side of the system inducing ascendent (anabatic) currents and to the trailing edge where the current speed is reduced, tending to be equal to the general speed at wake.

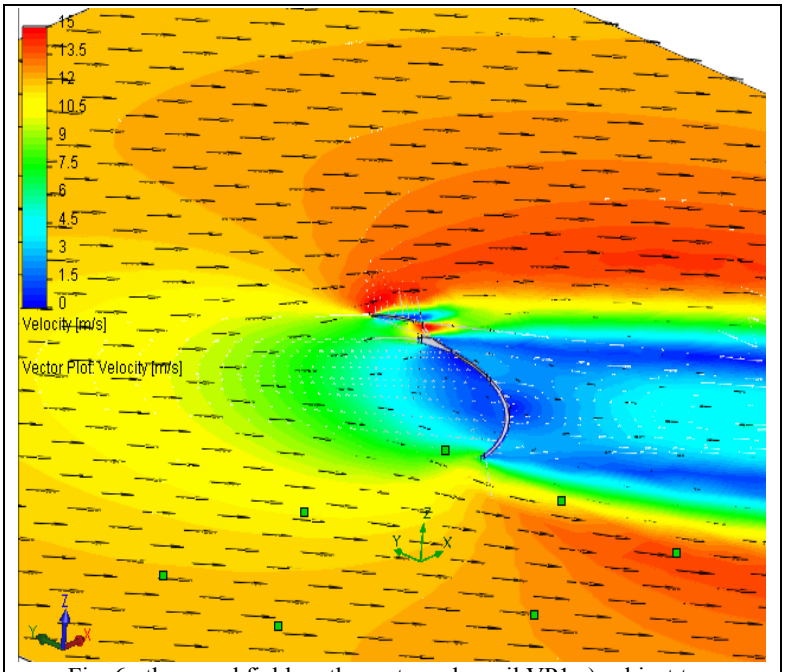

Fig. 6– the speed field on the rectangular sail VP1.a) subject to a flow/stream of 12m/s and an angle of attack of 45°

The influence of slat can be seen in Fig.6, because the current speed increased on the upper side of hybrid sail, from 12 m/s to 15 m/s, especially to the bow, where a very big difference of speed, from 15 m/s to 1.5 m/s, induces an accelerated flow determining a big difference of pressure and leading to an increase of propulsion.

As a conclusion, the finite element method applied to the sail aerodynamics allows to perform a rough cantitative study of the flows and the

pressure fields induced around the sail. The calculation programs using the finite element method, compute very many values showing the convergences obtained and plot by curves the behaviour of a studied sail in various situations.

Also, these programs allow a rough study on the sail's shape, from which we can draw some conclusions regarding the efficiency of the studied solution, as well as the change of the sail's shape according to different sailing points to the wind, and according to the wind speed for performing an optimum propulsion (a higher propelling force and a lower drift).

4. Test data

All the test were achieved in a constant and uniform flow, the air current speed being of 8m/s, (the current speed is permanently checked with an anemometer (wind-gauge/air meter).

The tests were performed in the wind tunnel of the Naval Academy in Constanta. In Fig 1 are presented the experimental model dimensions. The sliding step of the mast for determining the forces and the motion uses the principle of balance, being provided with pans for putting different weights for measuring forces, and in the centre of rotating plate is fitted the model of the hybrid sail. The test soft sails were made of dacron (a special sail cloth) and it was used a square sail with a hoist of 0.25m and a waft of 0,125m at its base and two slats with the dimensions conform Fig.1. A disadvantage of this tunnel was the boundary layer from the floor level, of about 0.03 cm which cannot be removed, but nevertheless, these conditions might be closer to reality, taking into account that at the sea level there is such a boundary layer due to friction between air and water surface.

4.1. The aerodynamical characteristics of the model and the influence of the hybrid wing aspect.

The aerodynamic characteristics on C_Z, C_X, for hybrid sails of different aspect are shown in Fig. 7 and 8, where an angle of the slat of $\omega = 35°$ and a boom angle of $\beta = 30°$ were used.

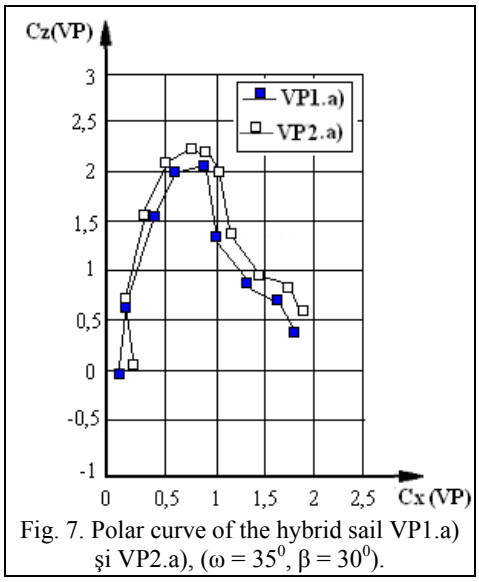

Fig. 7. Polar curve of the hybrid sail VP1.a) şi VP2.a), ($\omega = 35^0$, $\beta = 30^0$).

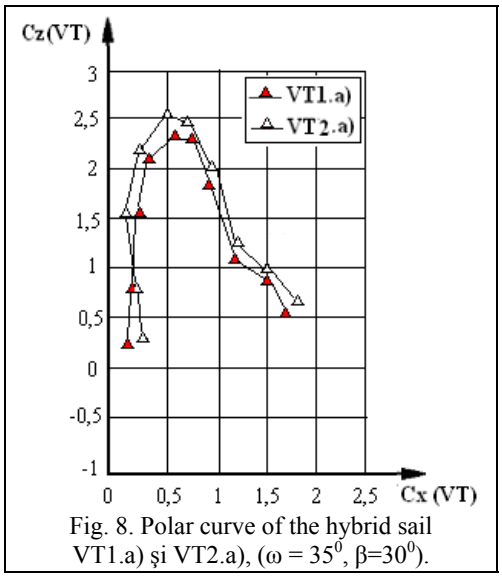

Fig. 8. Polar curve of the hybrid sail VT1.a) şi VT2.a), ($\omega = 35^0$, $\beta=30^0$).

In the train of the tests with the model in the wind tunnel resulted the polar curves of the hybrid-sails (Fig.7; 8) with square soft sail (VP), or triangular soft sail (VT), which leaded to the conclusion that large changes of the aspect ratio have small influence on the drag coefficients C_X both for VP and for VT sails, the drag depending mainly on the lateral shape of the hybrid-sail combinations.

The test results obtained show the maximum lifting force is registered at $(C_Z)max = 2$ in case of VP1.a), and at $(C_Z)max = 2,2$ in case of VP2.a); for VT1.a), at $(C_Z)max = 2,3$ and for VT2.a), at $(C_Z)max = 2,5$.

The slope of this lift-curve aquired from polar sails and the C_Z/C_X ratio are determinated to estabilish the sail performance, and in the hybrid-sail case with at leading edge slat, it resulted theoretical and practical that this performance is enlarget with appx. 50% in advance of regular sails.

At low incidences area (with respect to a.p.n.), that is small values of coefficient C_Z, the test errors are high, the soft sail can flap. Therefore, to comparison with theory, there were used certain higher values of the coefficient C_Z, the null(zero) lift angle being determined by linear regression.

Besides the data presented in this paper, many other aspects have been studied, such as: fineness of sail; effect of slat dimensions; effect of using multiple slot, etc.

5. Comparisons. Final conclusions.

The experimental,analytical and numerical data are presented in Table3 .

Table 3.

Experimental,analytical and numerical data

Model	Method	$\frac{dC_Z}{d\alpha_0}(grad^{-1})$	Force of propulsion [N]	Errors [%]	
				Slope	Force
VT 1 ($\alpha = 30^0$)	Experiment	0,0741	2,56	0.0	0.0
	Prop. analytical method	0,0751	2,59	1.33	1.17
	Finite elem. Method	--	3,05	--	19.14
VP 1 ($\alpha = 35^0$)	Experiment	0,0556	3,45	0.0	0.0
	Prop. analytical method	0,0614	3,1	10.43	10.14
	Finite elem. Method	--	4,4	--	27.53

From Table 3 one can see a good agreement between the proposed analytical method and experiment especially for wing systems with larger aspect ratios; the experimental values for the slope $\frac{dC_Z}{d\alpha_0}(grad^{-1})$ are smaller, possible due to the friction influence. One can notify as well that it was uncertain to determine the slope values by using the finite element technics via **CosmosFloWorks** code. A rough force determination is however possible by using this code.

R E F E R E N C E S

1. *Carafoli, E.,* „Aerodynamics" (in romanian), Ed.Tehnică, Bucureşti,1951 .
2. *Berbente C.*,"A method for the aerodynamical calculation of finite span wings in incompressible flow"(in romanian), Buletinul I.P.B. tom XXXV, nr.5, sept-oct.1973, pag.37-49.
3. *Maraloi, C.*," Modern solutions regarding the optimization of sail ship propulsion system", Bul.Şt.al Acad.Navale „Mircea cel Bătrân",vol.6, pp.37-46,2003.

4. *Maraloi, C*.," Experimental Researches for Determining the Propulsion Parameters of the Hybrid- sail Ships", Revue Roumaine des Sciences Techniques, Série de Mécanique Appliquée, tome 50, n^{o} 3-4, 2005.
5. *C. Berbente, C. Maraloi*, „Theoretical and Experimental Study regarding the Aerodynamics of a Ship Sail System", „Caius Iacob" Conference on Fluid Mechanics and its Applications, Bucharest, 25-26 November, 2005.